Electronic Supplementary Material (ESI) for Journal of Materials Chemistry C.

Supplementary Materials for

Low temperature and high performance ZnSnO thin film transistors engineered by in-situ thermal manipulation

Wengao Pan [a], Xiaoliang Zhou [a], Qingping Lin [a], Jie Chen [a] Lei Lu [a], Shengdong Zhang [a,b*],

[a] School of Electronic and Computer Engineering, Peking University, Shenzhen, 518055, China

[b] Institute of Microelectronics, Peking University, Beijing 100871, China

The Supplementary Materials include:

- Theoretical calculation methods.
- Fig. S1, Fig. S2 and Fig. S3.
- Table S1.
- References.

* Corresponding author.

E-mail address: zhangsd@pku.edu.cn (S.D. Zhang).

Theoretical calculation methods

Theoretical calculations were performed in Materials Studio software (BIOVIA Inc). Amorphous structural Zn_2SnO_4 (ZTO) model was built by molecular dynamics (MD) with Forcite module based on "melt and quench" method [1]. Firstly, 2×2×2 crystal ZTO supercell was geometrically optimized and then melt at 3000K for 1000ps with canonical ensemble (NVT), time step of 5fs, random initial velocity and classical force field. Afterward, the system was quickly quenched to 300K for 100ps with the similar simulation parameters except the initial velocity was changed to current. Finally, amorphous ZTO without oxygen vacancy was obtained, and ZTO structure with neutral oxygen vacancy was built by directly deleting a O atom, as shown in **Fig. S1**. The ZTO structure with doubly charged oxygen vacancy was modeled by further removing two charges from the supercell [2].

The properties were calculated by density functional theory (DFT) using CASTEP module [3]. The generalized gradient approximation (GGA) [4] and the Perdew-Burke-Ernzerhof revised for solid (PBEsol) [5] functional with OTFG ultrasoft pseudo-potentials [6] was adopted to investigate the exchange and correlation energies. The electronic configurations were ($3d^{10}4s^2$) for Zn, ($4d^{10}5s^25p^2$) for Sn, ($2s^22p^4$) for O, respectively. The energy bandgaps were uniformly corrected by scissors operator of 3 eV. The cutoff energy of plane wave basis set was 571.4 eV and the Monkhorst-Pack *k*-point grids were 2×2×2. The detailed convergence standards were as below: (1) Force tolerance was 0.03 eV/Å; (2) Total energy limits to 10^{-5} eV/atom; (3) Max stress tolerance was 0.05 GPa; (4) Max displacement tolerance was 0.001 Å; (5) self-consistent field (SCF) converges to 10^{-6} eV/atom.

Figures

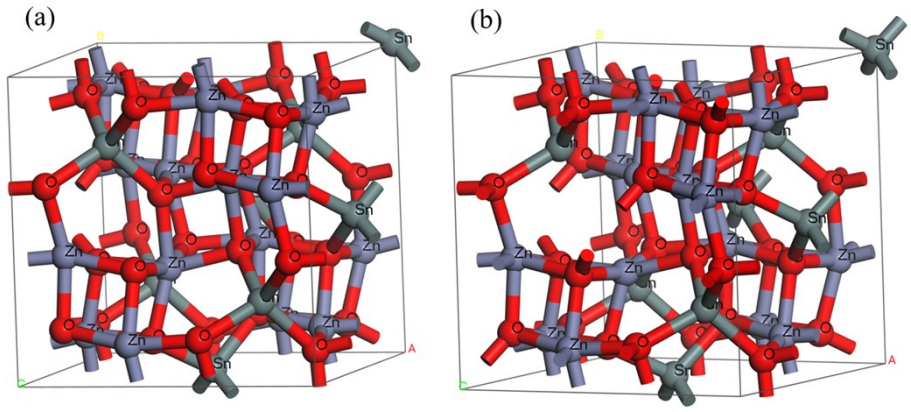

Fig. S1 The amorphous models of ZTO structure (a) without and (b) with oxygen vacancy built for DFT calculation.

Fig. S2 is the Local density of state (LDOS) of ZTO without oxygen vacancy and with different oxygen defect. The Fermi level is set with the energy of 0 eV, marked as dotted line. Generally, all the valence band maximum (VBM) are mainly composed of the electrons from O atom and Zn atom. all the conduction band minimum (CBM) are co-dominated by the electrons of all atoms, and the contribution order is Sn atom, O atom and Zn atom, respectively. It may be the another reason why the amount of Sn is much closely related to the electron transportation and the mobility than that of Zn, although both Sn^{4+} and Zn^{2+} possess the expected electron configuration (n-1)d^{10}ns^{0}(n$\geqslant$4), and the ion radius of the former is bigger than that of the later. Besides, the VBM of ZTO with neutral oxygen vacancy shifts towards lower energy direction compared with that of ZTO without oxygen vacancy, broadening the bandgap. No obvious movement of VBM and/or CBM are observed in ZTO with charged oxygen vacancy.

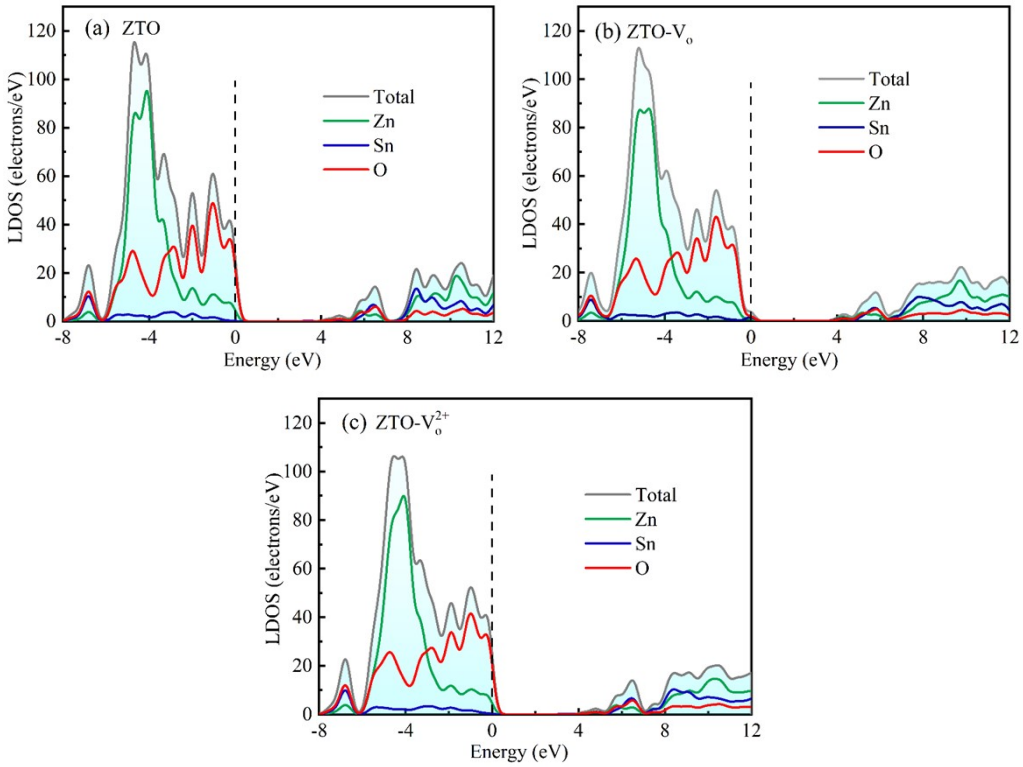

Fig. S2 LDOS of ZTO without oxygen vacancy (a), with neutral oxygen vacancy (b) and charged oxygen vacancy (c).

Fig. S3(a), **(b)** and **(c)** are the partial density of state (PDOS) of Zn atom, Sn atom and O atom, respectively. It can be concluded that, the electrons near VBM result from the Zn 3*d* orbit and O 2*p* orbit, and the latter is dominant. The electrons near VBM are contributed from the Sn 5*s* orbit and O 2*p* orbit and Zn 4*s* orbit, and the former two are primary. **Fig. S3(d)**, **(e)** and **(f)** are the direct PDOS contrasts of Zn 4*s*, Sn 5*s* and O 2*p*, respectively. Generally, no obvious discrepancies are observed in PDOS between ZTO without and with charged oxygen vacancy, while the PDOS of ZTO with neutral oxygen vacancy shows overall movement in Zn 4*d* orbit and O 2*p* orbit towards lower energy direction and a PDOS peak in Sn 5*s* orbit appears near Fermi level. It is worth noting that, in **Fig. S3(d)**, the PDOS of Sn 5*s* orbit of ZTO with charged oxygen vacancy is higher that of perfect ZTO, which may be the reason for the acceleration of electron transportation and the enhancement of mobility.

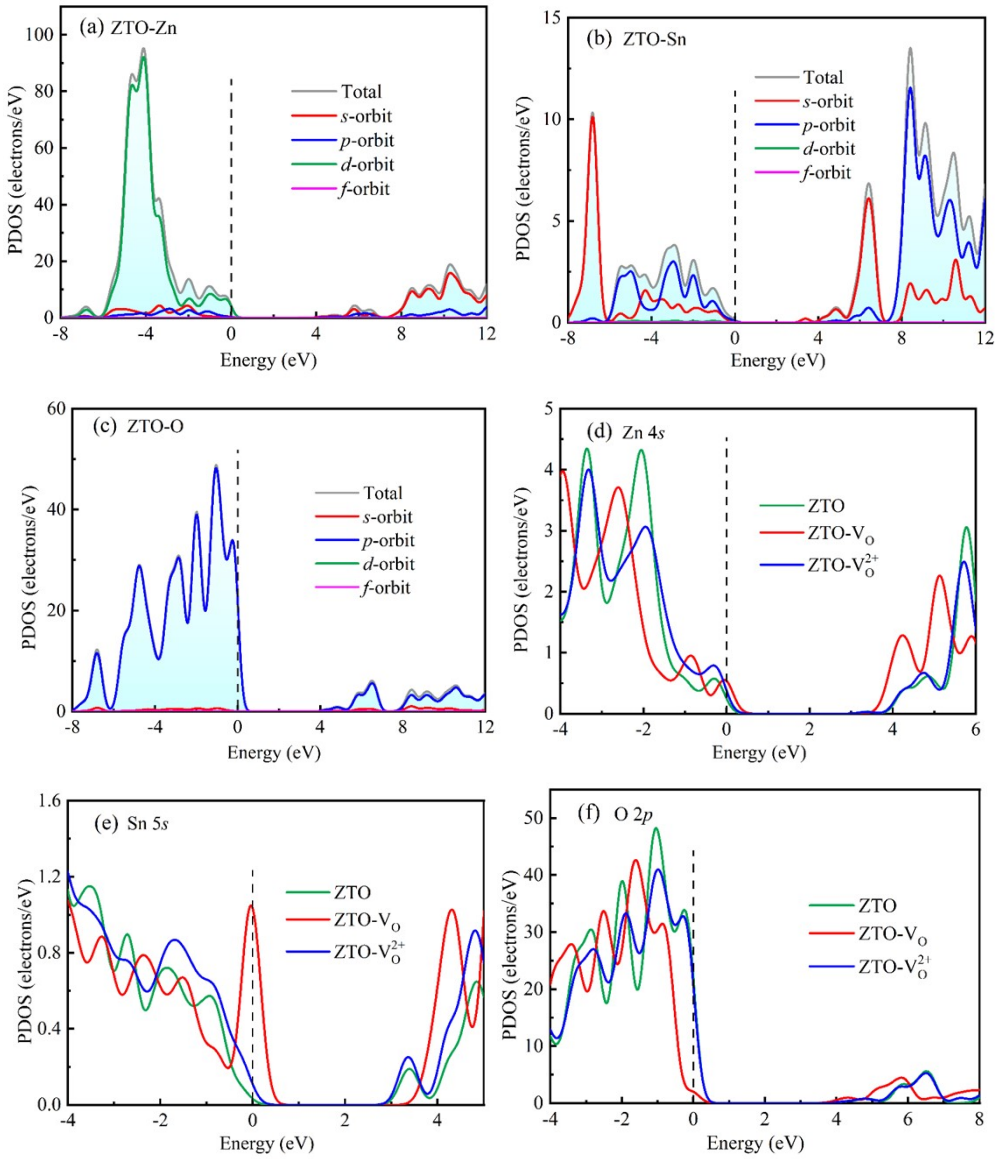

Fig. S3 Partial density of state (PDOS) of (a) Zn atom, (b) Sn atom and (c) O atom in ZTO supercell. The PDOS contrasts of (d)Zn 4*s* orbit, (e)Sn 5*s* orbit and (f)O 2*p* orbit in ZTO without oxygen vacancy and with different oxygen defects.

Tables

Table S1 Comparisons of processing temperature and field effect mobility berween this work and other ZTO related investigations.

Material systems	Processing temperature (℃)	Field effect mobility (cm^2/Vs)	References
ZTO	300	9.60	This work
ZTO	300	8.19	[7]
ZTO	250	2.00	[8]
ZTO	500	3.70	[9]
ZTO	400	13.20	[10]
ZTO	250	14.00	[11]
ZTO	350	10.70	[12]
ZTO	500	14.11	[13]
ZTO	400	5.50	[14]
ZTO	500	5.90	[15]
ZTO	500	8.76	[16]
ZTO	400	2.96	[17]
Al-ZTO	500	2.41	[18]
Al-ZTO	600	5.41	[19]
Al-ZTO	150	6.20	[20]
F-ZTO	350	7.93	[21]
Ga-ZTO	500	1.21	[22]
Hf-ZTO	400	1.15	[23]
Hf-ZTO	300	5.80	[24]
Li-ZTO	350	24.70	[25]
Li-N-ZTO	675	26.80	[26]
Mg-ZTO	400	0.27	[27]
N-ZTO	635	41.80	[28]
Nb-ZTO	480	5.32	[29]
Si-ZTO	400	1.00	[30]
Ta-ZTO	400	2.24	[31]
Ti-ZTO	600	0.52	[32]
Ti-ZTO	600	4.10	[33]

Zr-ZTO	500	4.02	[34]
Zr-ZTO	600	6.43	[35]

References

[1] K. Nomura, T. Kamiya, H. Ohta, T. Uruga, M. Hirano and H. Hosono, *Phys. Rev. B,* 2007, **75**, 035212.

[2] N. Raja, D. Murali, S.V.M. Satyanarayana and M. Posselt, *RSC Adv.,* 2019, **9**, 34158-34165.

[3] S.J. Clark, M.D. Segall, C.J. Pickard, P.J. Hasnip, M.I.J. Probert, K. Refson and M.C. Payne, *Z. Kristallogr.,* 2005, **220**, 567-570.

[4] J.P. Perdew, K. Burke and M. Ernzerhof, *Phys. Rev. Lett.,* 1998, **77**, 3865-3868.

[5] J.P. Perdew, A. Ruzsinszky, G.I. Csonka, O.A. Vydrov, G.E. Scuseria, L.A. Constantin, X.L. Zhou and K. Burke, *Phys. Rev. Lett.,* 2008, **100**, 136406.

[6] J. Tóbik and A.D. Corso, *J. Chem. Phys.,* 2004, **120**, 9934-9941.

[7] S.J. Oh, C.J. Han, J.W. Kim, Y.H. Kim, S.K. Park, J.I. Han, J.W. Kang and M.S. Oh, *Electrochem. Solid St.,* 2011, **14**, H354-H357.

[8] Y.H. Hwang, S.J. Seo, J.H. Jeon and B.S. Bae, *Electrochem. Solid St.,* 2012, **15**, H91-H93.

[9] X. Yang, S. Jiang, J. Li, J.H. Zhang and X.F. Li, *RSC Adv.,* 2018, **8**, 20990-20995.

[10] B.D. Ahn, D. Choi, C. Choi and J.S. Park, *Appl. Phys. Lett.,* 2014, **105**, 092103.

[11] W.B. Jackson, R.L. Hoffman and G.S. Herman, *Appl. Phys. Lett.,* 2005, **87**, 193503.

[12] H.W. Lee, B.S. Yang, Y.J. Kim, A.Y. Hwang, S. Oh, J.H. Lee, J.K. Jeong and H.J. Kim, *IEEE T Electron. Dev.,* 2014, **61**, 3191-3198.

[13] S.J. Seo, C.G. Choi, Y.H. Hwang and B.S. Bae, *J. Phys. D: Appl. Phys.,* 2009, **42**, 035106.

[14] M. Fakhri, P. Görrn, T. Weimann, P. Hinze and T. Riedl, *Appl. Phys. Lett.,* 2011, **99**, 123503.

[15] Q. Zhang, G.D. Xia, L.B. Li, W.W. Xia, H.Y. Gong and S.M. Wang, *Curr. Appl. Phys.,* 2019, **19**, 174-181.

[16] Y.S. Rim, D.L. Kim, W.H. Jeong and H.J. Kim, *Electrochem. Solid. St.,* 2012, **15**, H37-H40.

[17] W.S. Choi, *Electron. Mater. Lett.,* 2019, **15**, 171-178.

[18] H.J. Jeon, W.J. Maeng and J.S. Park, *Ceram. Int.,* 2014, **40**, 8769-8774.

[19] Y.G. Lee and W.S. Choi, *Electron. Mater. Lett.,* 2013, **9**, 719-722.

[20] D.H. Cho, S. Yang, C. Byun, J. Shin, M.K. Ryu, S.H. Park, C.S. Hwang, S.M. Chung, W.S. Cheong, S.M. Yoon and H.Y. Chu, *Appl. Phys. Lett.,* 2008, **93**, 142111.

[21] J.H. Jeon, Y.H. Hwang, J.H. Jin and B.S. Bae, *MRS Commun.,* 2012, **2**, 17-22.

[22] Y. Jeong, K. Song, T. Jun, S. Jeong and J. Moon, *Thin Solid Films,* 2011, **519**, 6164-6168.

[23] J.Y. Choi, S.S. Kim and S.Y. Lee, *Appl. Phys. Lett.,* 2012, **100**, 022109.

[24] C.X. Huang, J. Li, Y.Z. Fu, J.H. Zhang, X.Y. Jiang, Z.L. Zhang and Q.H. Yang, *J. Alloy Compd.,* 2016, **681**, 81-87.

[25] J.H. Lim, H.J. Jeong, K.T. Oh, D.H. Kim, J.S. Park and J.S. Park, *J. Alloy Compd.,* 2018, **762**, 881-886.

[26] S.Q. Dai, T. Wang, R. Li, D.Z. Zhou, Y.F Peng, H.L. Wang, X.Q. Zhang and Y.S. Wang, *Ceram. Int.,* 2007, **43**, 4926-4929.

[27] H.B. Kim and H.S. Lee, *Thin Solid Films,* 2014, **550**, 504-508.

[28] S.Q. Dai, T. Wang, R. Li, Q. Wang, Y.B. Ma, L.J. Tian, J.B. Su, Y. Wang, D.Z. Zhou, X.Q. Zhang and Y.S. Wang, *J. Alloy Compd.,* 2018, **745**, 256-261.

[29] J.S. Jeng, *J. Alloy Compd.,* 2016, **676**, 86-90.

[30] C.J. Wu, X.F. Li, J.G. Lu, Z.Z. Ye, J. Zhang, T.T. Zhou, R.J. Sun, L.X. Chen, B. Lu and X.H. Pan, *Appl. Phys. Lett.,* 2013, **103**, 082109.

[31] X.W. Sun, M. Zhang, K.L. Song, L. Wei, Y.F. Yin and X. Zhang, *Thin Solid Films,* 2020, **709**, 138135.

[32] J.C. Do, C.H. Ahn, H.K. Cho and H.S. Lee, *J. Phys. D: Appl. Phys.,* 2012, 45, 225103.

[33] J.C. Do and H.B. Kim, *J. Mater. Res.,* 2012, **27**, 2293-2298.

[34] Y.S. Rim, D. L. Kim, W.H. Jeong, S.J. Kim, B.S. Kim and H.J. Kim, *Curr. Appl. Phys.,* 2011, **11**, S258-S261.

[35] H. Kim and W. Choi, *Ceram. Int.,* 2017, **43**, 4775-4779.